

- (15) Flory, P. J.; Mark, J. E.; Abe, A. *J. Am. Chem. Soc.* **1966**, *88*, 639.
(16) Mark, J. E. *J. Chem. Phys.* **1968**, *49*, 1398.
(17) Stern, S. A.; Shah, V. M. and Hardy, B. J. *J. Polym. Sci., Polym. Phys. Ed.* **1987**, *25*, 1263.
Registry No. CO₂, 124-38-9; CH₄, 74-82-8; C₃H₈, 74-98-6.

Molecular Weight and Comparative Studies of Poly-3- and Poly-4-BCMU Monolayers and Multilayers

J. E. Biegajski, R. Burzynski, D. A. Cadenhead,* and P. N. Prasad*

Department of Chemistry, State University of New York at Buffalo,
Buffalo, New York 14214. Received January 10, 1989;
Revised Manuscript Received July 13, 1989

ABSTRACT: The molecular weights of three poly-4-BCMU samples were determined with a film balance technique by assuming near ideal behavior at low film concentrations. For the high, medium, and low molecular weight samples the number-average molecular weights were 410 000, 300 000, and 66 000 g/mol, respectively. All three samples showed a monolayer/bilayer, yellow coil/red rod conformational change similar to those we previously reported;¹ however, the low molecular weight sample initiated the compressional transition at a significantly lower area/residue than did either the medium or high molecular weight samples. This was interpreted to mean that the shorter chains in the low molecular weight sample had an increased number of semisoluble end groups. The visible absorption spectra indicated that while the low molecular weight sample underwent a yellow coil/red rod transition more readily and to a greater extent, the resultant red rod form was somewhat less organized. We have also made further comparisons of poly-3- and poly-4-BCMU. A reevaluation of the thermodynamics of the monolayer/bilayer transition, as indicated by surface pressure/area per residue isotherms, using a modified Clapeyron equation, showed slight exothermicity and increasing order accompanying multilayer formation of red rod poly-4-BCMU. Resonance-enhanced, laser Raman spectroscopy clearly reveals that the upper layer of the condensed bilayer consists of the red rod form but that the residual lower layer remains in the yellow coil form. Transmission electron microscopy of both poly-3-BCMU and poly-4-BCMU reveals a transition from a smooth surface in the monolayer region to one exhibiting numerous rodlike features in the transition region until in the condensed phase a more uniform but textured appearance is achieved. The effects of both solid and aqueous substrates were also examined. Deposition of monolayers of both polymers on hydrophobic solid substrates gave clear visible spectroscopic evidence of a small, partially induced coil to rod transition, in contrast to similar monolayers deposited on hydrophilic solid surfaces. Changing the pH and the addition of both sodium and calcium ions to an aqueous substrate also had significant effects. For poly-4-BCMU high pH (12.5) values resulted in an overall expansion for both expanded and condensed isotherm segments. For poly-3-BCMU the condensed state was expanded but the expanded (monolayer) state was condensed. A combination of ionization and hydrolysis was invoked for both polymers with ionization predominating for poly-4-BCMU and hydrolysis playing a more significant role for poly-3-BCMU. Calcium ions were shown to greatly condense ionized films while high concentrations of sodium ions produced expansion. The latter resulted in nearly identical compressional isotherms for poly-3-BCMU and poly-4-BCMU, except for a shift of the highly sensitive transition region.

Introduction

Previously we have demonstrated that monolayers of both poly-4-BCMU¹ [poly(dibutyl 4,19-dioxo-5,18-dioxo-3,20-diaza-10,12-docosadienedioate)] and poly-3-BCMU² [poly(dibutyl 4,17-dioxo-5,16-dioxo-3,18-diaza-9,11-eicosadienedioate)] have surface pressure (π)-area per residue (A) isotherms exhibiting a phase transition that incorporates an intramolecular conformational transition from an expanded monomolecular amphipathic yellow coil form to a condensed multimolecular nonamphipathic red or blue rod form. The conformational transition, from coil to rod, has been previously reported, both in solution and solid-state films by others³⁻⁸ and has been interpreted as representing an increased effective π -electron conjugation length along the polymer backbone. The transition is brought about either by changing the solvent toward a more nonpolar composition or by decreasing the temperature. This allows intramolec-

ular hydrogen bonding to take place between adjacent side groups of the same polymer chain.

In this paper we report and compare the monomolecular film behavior of high and low molecular weight (MW) poly-4-BCMU samples. We will see that these show similar but somewhat different behavior from that of a medium MW poly-4-BCMU¹ through both π - A isotherms at the air/water interface and visible absorption spectra of Langmuir-Blodgett (LB) transferred films.

The number-average molecular weights of high, low, and previously studied medium MW samples of poly-4-BCMU were determined by using a film balance and a modified ideal gas law type equation, which applies at low surface pressures. π - A isotherms for medium MW poly-4-BCMU along with visible absorption spectra of LB transferred films are presented. Resonance Raman spectra of medium MW poly-4-BCMU transferred films provide complimentary evidence of the coil to rod conformational transition.

The relaxation observed between a continuous compression and a stepwise, "equilibrium" isotherm of poly-

* To whom correspondence should be addressed.

4-BCMU was also studied. Transmission electron microscopy of LB transferred films of both poly-4-BCMU and poly-3-BCMU reveal rodlike domains that exist in both the transition region and condensed multimolecular state, while the expanded monomolecular state film shows only a flat featureless topography lacking such domains.

The effect of a low-energy hydrophobic solid surface on the conformation of horizontally lifted poly-4-BCMU and poly-3-BCMU monolayers was studied by visible absorption spectroscopy. The hydrophobic surface was apparently able to induce increased order in films transferred in the expanded state and, to a lesser degree, the condensed state of both poly-4-BCMU and poly-3-BCMU.

The role of subphase pH and cation composition (i.e., Na^+ , Ca^{2+}) in determining the monolayer behavior of poly-4-BCMU and poly-3-BCMU were also studied. Both polymers showed monolayer behavior consistent with an ionized state and/or hydrolysis at elevated pH (pH 12.5). Addition of Ca^{2+} to the subphase (10^{-3} M CaCl_2) was followed by a marked condensation. In contrast an overall expansion of both poly-4-BCMU and poly-3-BCMU was obtained when films of these substances were spread on a 3.0 M NaCl subphase. On such a subphase the films of both showed near coincident π -A isotherms for all areas except within the transition region, where different pressures at the compressional initiation of the transition (π_t) reflected residual film differences.

Experimental Section

Surface pressure (π) versus area per residue (A) isotherms were obtained by using a Langmuir film balance, which has been described previously.⁹

Continuous compressional isotherms were obtained at a compressional speed of $10 \text{ \AA}^2 \text{ residue}^{-1} \text{ min}^{-1}$. Stepwise isotherms were determined through a series of short compressions followed by a waiting period (typically 10–15 min) until all relaxation had apparently ceased. Surface pressure was measured by the Wilhelmy plate method using a hydrogen fluoride, vapor-etched, glass coverslip and an automatic-nulling R.G. Cahn electrobalance and an analog chart recorder. Langmuir–Blodgett vertical film transfer was carried out by using a motorized screw-driven lift mechanism while a second, servo-driven motor adjusted a Teflon barrier in order to maintain a constant surface pressure ($\pm 0.1 \text{ dyn/cm}$). Horizontally lifted films were transferred by lowering a hydrophobic substrate parallel to the film-covered interface until contact was achieved, at which time any remaining film surrounding the slide was suctioned off by a pipet connected to an aspirator. The slide with the adherent monolayer film was then carefully removed from the interface.

All glass slides used as substrates were cleaned by first immersing them in hot chromic acid for 12 h. This was followed by a thorough rinsing of the slides with singly distilled water and then with quadruply distilled water. The slides to be used for vertical transfers (with an original hydrophilic surface) were then treated for approximately 5 min in an argon plasma prior to use. Those slides used for horizontal transfers (with a hydrophobic surface) were first cleaned as above and then alkylated by immersing them in a dilute solution of octadecyltrichlorosilane (OTS) in chloroform (0.1 mL of OTS in 50 mL of CHCl_3) for approximately 10 min, after which they were rinsed with chloroform and quadruply distilled water and then finally dried in a stream of nitrogen.

Subphase water was first distilled and then deionized to give a resistivity of at least $15.0 \text{ M}\Omega \text{ cm}$. This water was then quadruply distilled, first from an alkaline stage, then from an acidic stage, and finally twice from an all-quartz still. Both NaOH and CaCl_2 were used as supplied without further purification for isotherm determination since neither gave an indication of surface-active impurities ($< 0.1 \text{ dyn/cm}$). For the molecular weight determinations, where precise low-pressure measurements are required, the NaCl used in its subphase was roasted at 540°C

for 12 h to remove any possible trace of organic material. The chloroform used as a spreading solvent was purified by first passing it through an alumina column and then by distillation.

The high and low molecular weight samples were obtained by adding an equivalent amount of a nonpolymer solvent (hexane) to a saturated chloroform solution of a medium molecular weight sample. Addition of the nonsolvent resulted in an aggregation of the high molecular weight sample, which was centrifuged off. The low molecular weight sample was then recovered from the remaining solution.

The films used for transmission electron microscopy were first vertically transferred onto hydrophilic freshly cleaved mica substrates. These transferred films were then shadow cast under vacuum ($\sim 10^{-4}$ torr) using as the filament a 2.5-cm length of Pd/Pt (4:1) wire that was evaporated at an angle of approximately 20° . This resulted in a metal deposited thickness of approximately 23 \AA . This was followed by a rotary carbon shadowing to give the underlying Pd/Pt layer sufficient mechanical strength to float the resultant two-layer sandwich onto a water surface in order to allow for mounting onto copper electron microscope grids (400 mesh). After air drying the mounted films were viewed and photographed with a JEOL 100-EX transmission electron microscope.

Visible absorption spectra were obtained on a Shimadzu UV 260 UV-visible spectrophotometer. All films were transferred and spectra obtained at temperatures between 20 and 25°C .

Results and Discussion

(a) Molecular Weight Determination. Number-averaged molecular weights of samples of poly-4-BCMU were determined by using a film balance to measure the low surface pressure region of the π -A isotherm ($\pi < 0.2 \text{ dyn/cm}$). The molecular weights were obtained by plotting the function $\pi(A - A_0)$ versus π , and extrapolating to $\pi = 0$, assuming a modified ideal gas law of the form

$$\pi(A - A_0) = RT/M_N \times 10^3 \quad (1)$$

where π = surface pressure in ergs per centimeter cubed, A = available surface area per milligram of polymer, A_0 = the surface area occupied by one milligram of the close-packed polymer, R = the gas constant in ergs/mol·K, T = the absolute temperature in kelvin, and M_N = the number-average molecular weight of the polymer in grams per mole. It is possible to calculate M_N from the intercept as $\pi \rightarrow 0$. For poly-4-BCMU we take A_0 to be equal to $13\,200 \text{ cm}^2/\text{mg}$ based on CPK space-filling models. The data for both high and low MW poly-4-BCMU are shown in Figure 1. The subphases used were 1.4 and 2.8 M NaCl in order to reduce the effects of slight polymer solubility as indicated by preliminary studies on water at 24.3°C . Plots for both samples show positive deviations from ideal behavior (i.e., $d(\pi(A - A_0))/d\pi > 0$) and show deviations from linearity over the higher pressure range studied. This occurred to a lesser degree with the 2.8 M NaCl subphase in which the polymer had the lowest solubility. The high MW sample was found to give an M_N equal to $410\,000 \text{ g/mol}$, while the low MW sample gave an M_N equal to $66\,000 \text{ g/mol}$. This gives a ratio of 6.2 for $M_N(\text{high})/M_N(\text{low})$. Thus, on average, there would be 6.2 times as many chain ends in the case of low MW poly-4-BCMU than for the high MW poly-4-BCMU with equivalent quantities of polymer. Such chain ends will inevitably have some kind of dipole moment associated with them and have greater flexibility than chain loops. It should presumably be easier to submerge a chain end than a chain loop at the air/water interface, and this could explain the more condensed expanded state observed for low MW poly-4-BCMU. The molecular weight of the medium MW poly-4-BCMU sample was $300\,000 \text{ g/mol}$. The data are not shown here in the interest of figure clarity. Due to difficulties in mea-

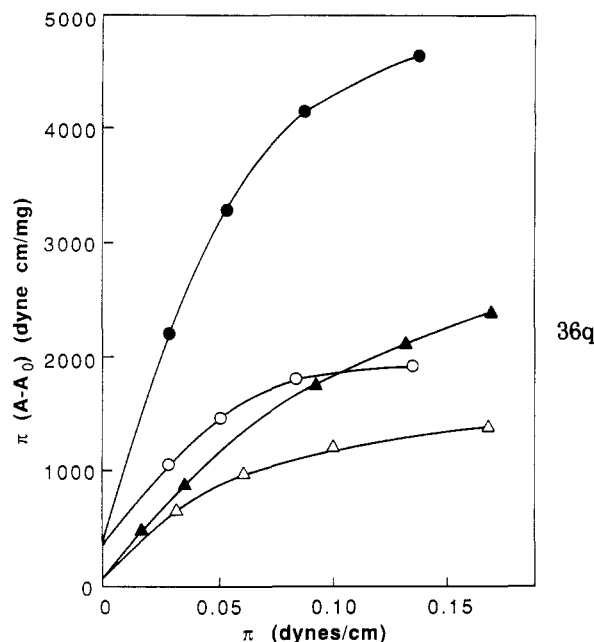


Figure 1. Surface pressure (dyn/cm) versus area per residue (\AA^2) isotherms for a high molecular weight sample (Δ) and a low molecular weight sample (\square) of poly-4-BCMU compressed at the air/water interface.

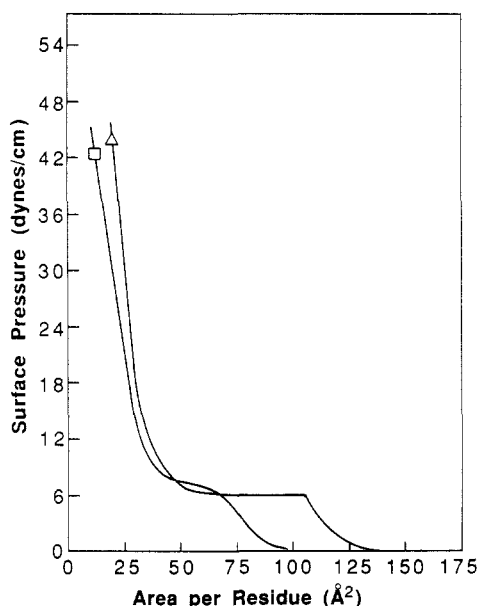


Figure 2. Molecular weight determination for high and low molecular weight poly-4-BCMU samples on 1.4 M and 2.8 M NaCl aqueous subphases: (Δ) 1.4 M, high; (\circ) 1.4 M, low; (\blacktriangle) 2.8 M, high; (\bullet) 2.8 M, low. Molecular weights reported were for 2.8 M NaCl subphases. Ordinate: $\pi(A - A_0)$ in dyn cm mg^{-1} , where A_0 is the close-packed area/residue. Abscissa: π in dyn cm^{-1} .

suring extremely low surface pressures, the molecular weight values should be taken as having a standard deviation of $\pm 10\,000$ g/mol.

(b) High and Low MW Poly-4-BCMU. The surface pressure (π) versus area per residue (A) isotherms of both a high and low molecular weight sample of poly-4-BCMU are shown in Figure 2. While both exhibit a phase transition similar to that previously observed for medium MW poly-4-BCMU monolayers at the air/water interface,¹ the low MW sample is clearly more condensed, particularly in the monolayer region, than either the high MW or medium MW sample. The fact that the length of the transition region (ΔA) for the low MW sample is

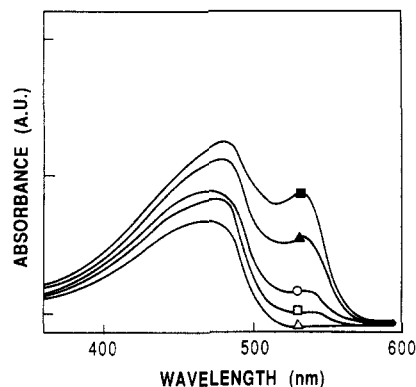


Figure 3. Visible absorption spectra of LB vertically transferred single-layer films of high molecular weight poly-4-BCMU samples corresponding to five different surface pressures in the expanded state, below the transition ($\pi_t - 1$ dyn/cm) (Δ), at the start of the transition (\square), at the finish (\circ) of the transition (π_t dyn/cm), and above the transition ($\pi_t + 1.5$ dyn/cm) (\blacktriangle) and ($\pi_t + 5$ dyn/cm) (\blacksquare).

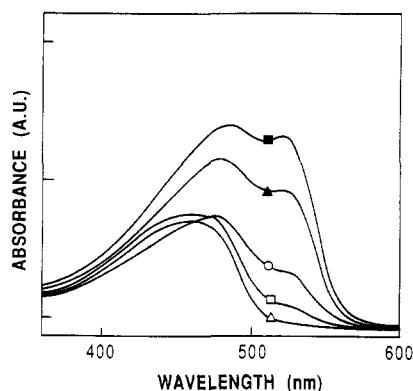


Figure 4. Visible absorption spectra of LB vertically transferred single-layer films of low molecular weight poly-4-BCMU samples corresponding to five different surface pressures: in the expanded state, below the transition ($\pi_t - 1$ dyn/cm) (Δ), at the start of the transition (\square), at the finish (\circ) of the transition (π_t dyn/cm), and above the transition ($\pi_t + 1.5$ dyn/cm) (\blacktriangle) and ($\pi_t + 5$ dyn/cm) (\blacksquare).

about one-half that of the high MW sample is due mainly to the large decrease in the area at the transition onset ($68 \text{ \AA}^2/\text{residue}$ for the low MW sample compared to $106 \text{ \AA}^2/\text{residue}$ for the high MW one), since the extrapolated area at zero pressure of the transition end point is 34 \AA^2 for both high and low MW samples. The compressibility of the condensed state of low MW poly-4-BCMU is somewhat greater than that of the high MW sample; however, the expanded states of both samples have compressibilities that are nearly equal. The transition region of the low MW sample has a finite slope compared to the nearly horizontal transition region of the medium and high MW samples.

The visible absorption spectra of LB vertically transferred, single-layer films corresponding to four different surface pressures from both high and low MW samples are shown in Figures 3 and 4, respectively. Both sets of spectra show the disordered yellow coil to be the predominant conformation of films transferred in the expanded state ($\pi_t - 1.0$ dyn/cm). Once in the transition region (π_t), evidence of the ordered red rod conformation begins to appear in the spectra as a shoulder at approximately 530 nm. At the low area/residue end of the transition there is, in addition to increased amounts of rod form, a decrease in absorbance associated with the coil form and a shift to longer wavelength. This wavelength shift is

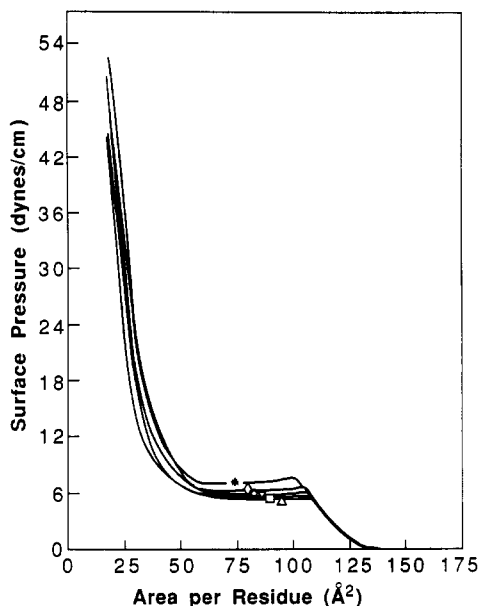


Figure 5. Surface pressure versus area per residue isotherms for the medium weight poly-4-BCMU sample at (*) 2.7, (◇) 10.0, (▽) 20.0, (□) 30.0, and (Δ) 37.0 °C. Isotherms were determined by continuous compression.

evidence that the amphipathic lower layer coil monolayer is becoming increasingly modified by the upper layer rod form as the phase transition progresses. Once beyond the end of the transition region and into the condensed state ($\pi_t + 1.5$ dyn/cm) the λ_{\max} of the yellow coil form of the high MW sample maintains its position, while that of the low MW sample continues to shift to longer wavelength. Finally, at a point well into the condensed state ($\pi_t + 5.0$ dyn/cm), the low MW yellow coil λ_{\max} again shifts to longer wavelength but the high MW coil λ_{\max} remains fixed.

All spectra showing both yellow coil and red rod forms appear more resolved for the high MW sample than for the low MW spectra. The wavelength separation between the coil and rod λ_{\max} for the high MW sample is approximately 60 nm, but it is only 40 nm for the low MW sample. Finally, the conversion of yellow coil to red rod form appears to be easier for the low MW sample than for the high MW sample at corresponding values of surface pressure above π_t . These differences suggest that increased polymer chain length seems to stabilize the interfacial amphipathic yellow coil form in monomolecular and LB films of poly-4-BCMU. Alternatively the higher MW sample has greater difficulty in undergoing the transition to the rod form. The spectra of solution-cast films of high and low MW poly-4-BCMU are seen to be almost identical, showing the predominance of the red rod form in both.

(c) Medium MW Poly-4-BCMU. π -A isotherms for medium MW poly-4-BCMU are shown in Figure 5 and are very similar to those previously reported.¹ The phase transition is observed over the entire temperature range studied (2.7–37.0 °C) and displays a negative temperature dependency ($d\pi_t/dT = -0.048$ dyn/cm·°C). The onset of the transition is marked by a small irreversible peak whose magnitude increases with decreasing temperature. π_t is taken as the pressure of the near-horizontal transition region. As can be seen in Figure 6, a plot of π_t versus T is nonlinear, particularly at lower temperatures, being essentially linear at higher temperatures. As reported previously,² the ΔH associated with the phase transition via a modified two-dimensional analogue of the

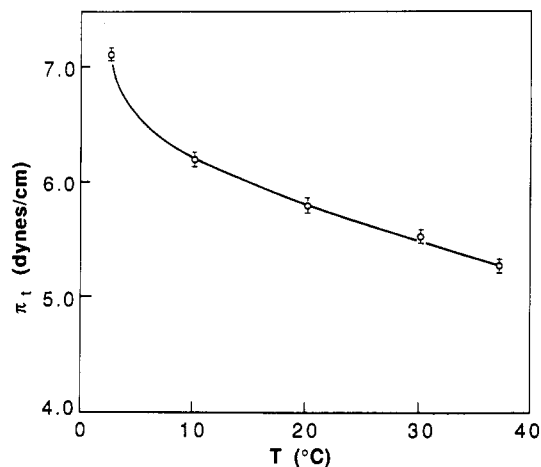


Figure 6. Transition pressure π_t in dynes per centimeter as a function of temperature in degrees Celsius for medium molecular weight poly-4-BCMU.

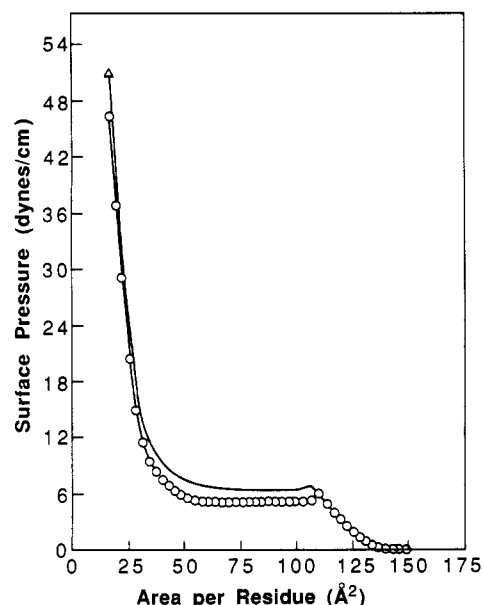


Figure 7. Comparison of a continuous compression (—) and a stepwise compressional isotherm (O) for medium molecular weight poly-4-BCMU.

Claperyon equation¹⁰

$$\Delta H = \left(\frac{d\pi_t}{dT} - \frac{\partial \gamma^\circ}{\partial T} \right) T \Delta A \quad (2)$$

gives $\Delta H = -3.1$ kcal/mol and $\Delta S = -11.4$ cal/deg·mol at 19.0 °C.

The difference observed between a continuous compression and a point by point stepwise isotherm of poly-4-BCMU is shown in Figure 7. While the expanded states are coincident, both the transition and condensed regions show appreciable relaxation. The initial nucleation of the condensed phase appears particularly difficult even with extended point by point isotherm determination. The slight exothermicity and entropy loss of the process reflect the competition between the formation of the more structured final form and the energy required to disrupt the initial monolayer. The magnitudes of the ΔH and ΔS values are consistent with the poly-4-BCMU red rod being slightly less ordered than the poly-3-BCMU blue rod form.^{1,2} In a previous evaluation of these thermodynamic quantities¹ the transition appeared endothermic when an uncorrected Claperyon equation was used. This emphasizes the significance of the $d\gamma^\circ/dT$ term.

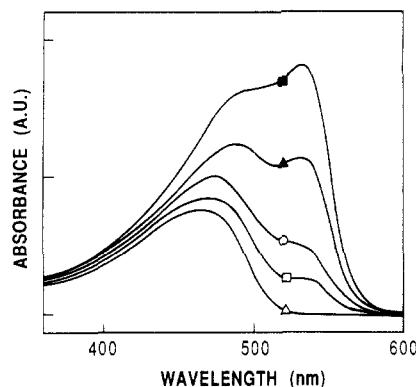


Figure 8. Visible absorption spectra of single-layer LB films of medium molecular weight poly-4-BCMU transferred at surface pressures (dyn/cm) below and above the transition pressure π_t : (Δ) ($\pi_t - 1$), (\square); (π_t , start of the transition); (\circ) (π_t , end of the transition); (\blacktriangle) ($\pi_t + 1.5$); (\blacksquare) ($\pi_t + 5.0$).

Visible absorption spectra of single-layer LB films of medium weight poly-4-BCMU transferred at five points along the isotherm are shown in Figure 8. Conversion from the yellow coil to the red rod form on proceeding from the expanded state through the transition to the condensed state is clearly seen, together with the shifting of the coil λ_{\max} from its initial value of 465 nm to its final value of 485 nm. While medium MW poly-4-BCMU behaves in a qualitatively similar fashion to high MW poly-4-BCMU in terms of its π -A isotherm, the medium MW sample still shows greater percent conversion to the red form on achieving a condensed state ($\pi_t + 5.0$ dyn/cm). In addition, it shows greater conversion than the low MW sample. One explanation is that a broader distribution of chain lengths in the medium MW sample may well lead to more packing defects in the transition state, thereby facilitating the formation of the rod form in an upper layer. Thus the presence of shorter chains among much longer ones would appear to greatly ease the yellow to red transition of the latter with the resultant red rod form being very similar to that formed by the more uniform high MW form.

(d) Raman Spectroscopy. A Raman spectrum of poly-4-BCMU LB film transferred on glass substrates within the plateau region is shown in Figure 9A. Two strong transitions were observed at 2115 and 1519 cm^{-1} . The main features of poly-4-BCMU LB film spectra are not substantially different from those of other polydiacetylenes.^{1,2} Therefore, we can tentatively assign the poly-4-BCMU Raman vibrations at 2115 and 1519 cm^{-1} to the polymer backbone stretching motions, $\nu_1(\text{C}\equiv\text{C})$, and $\nu_2(\text{C}=\text{C})$, respectively. Surprisingly for a diacetylenic polymer, the usually medium-intensity ν_3 vibration (in-plane deformation) at above 1200 cm^{-1} did not show up in poly-4-BCMU spectra. Instead we observed very weak bands at 1075 and 1039 cm^{-1} . The Raman frequencies reported here of a highly conjugated diacetylene polymer (the absorption spectra indicate a rodlike, planar structure) are somewhat higher than observed for other diacetylene polymers, for instance, poly-3-BCMU. Actually, our data are much closer to the values of the yellow form of the poly-3-BCMU in solution (ν_1 at 2120 cm^{-1} and ν_2 at 1520 cm^{-1}) than to the blue solution (ν_1 at 2084 cm^{-1} and ν_2 at 1460 cm^{-1}).³ This may well indicate the effect of the number of methylene ($-\text{CH}_2-$) groups on the molecular structure.³ In poly-4-BCMU, the formation of a hydrogen bond network possibly distorts the $(\text{CH}_2)_4$ linkage as well as the polymer chain. Such distortion can decrease the conjugation length of the polymer chain, which

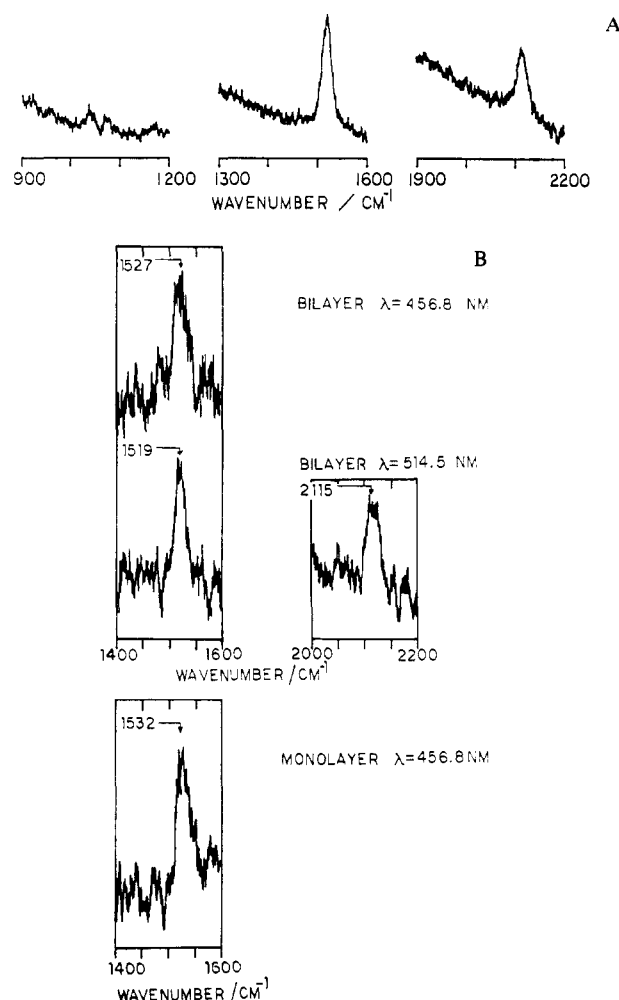


Figure 9. (A) Laser Raman spectrum of medium molecular weight poly-4-BCMU LB film transferred to a glass substrate when the film was at the compressional end of the monolayer/bilayer transition. The excitation wavelength was 532 nm with a spectral band-pass of the monochromator of 6 cm^{-1} . (B) Laser Raman spectra of a single bilayer film of poly-4-BCMU on a glass substrate using exciting frequencies of 456.8 and 514.5 nm and the spectrum of a monolayer of the same substance on a glass waveguide.

in turn may result in a shift of Raman frequencies toward higher values.

The spectra presented here were obtained with the incident laser energy coincident with the electronic states of the red polymer form (532 nm). In such a case Raman scattering is resonance enhanced and it is possible to detect Raman signals from single molecular layers. Thus, if our assumption of mixed yellow-red character for a bilayer film from the region within the plateau is correct, by selecting a laser wavelength to coincide with the yellow phase energy we should be able to monitor vibrational transitions of the coil form of the polymer. Figure 9B depicts the resonance Raman spectra of a single bilayer film of poly-4-BCMU recorded for 456.8 and 514.5 nm exciting laser frequencies (top right and left curves, respectively). The corresponding ν_2 bands are located at 1527 cm^{-1} (456.8-nm laser line) and 1519 cm^{-1} (514.5-nm laser line). The bottom curve in Figure 9B represents the Raman spectrum of a monolayer film of poly-4-BCMU transferred to a waveguide at an area/residue greater than those of the π -A isotherm plateau. As we mentioned earlier, the electronic spectra of such films are characteristic of the yellow polymer form, with an absorption maximum at ~ 470 nm. Therefore, by turning the laser

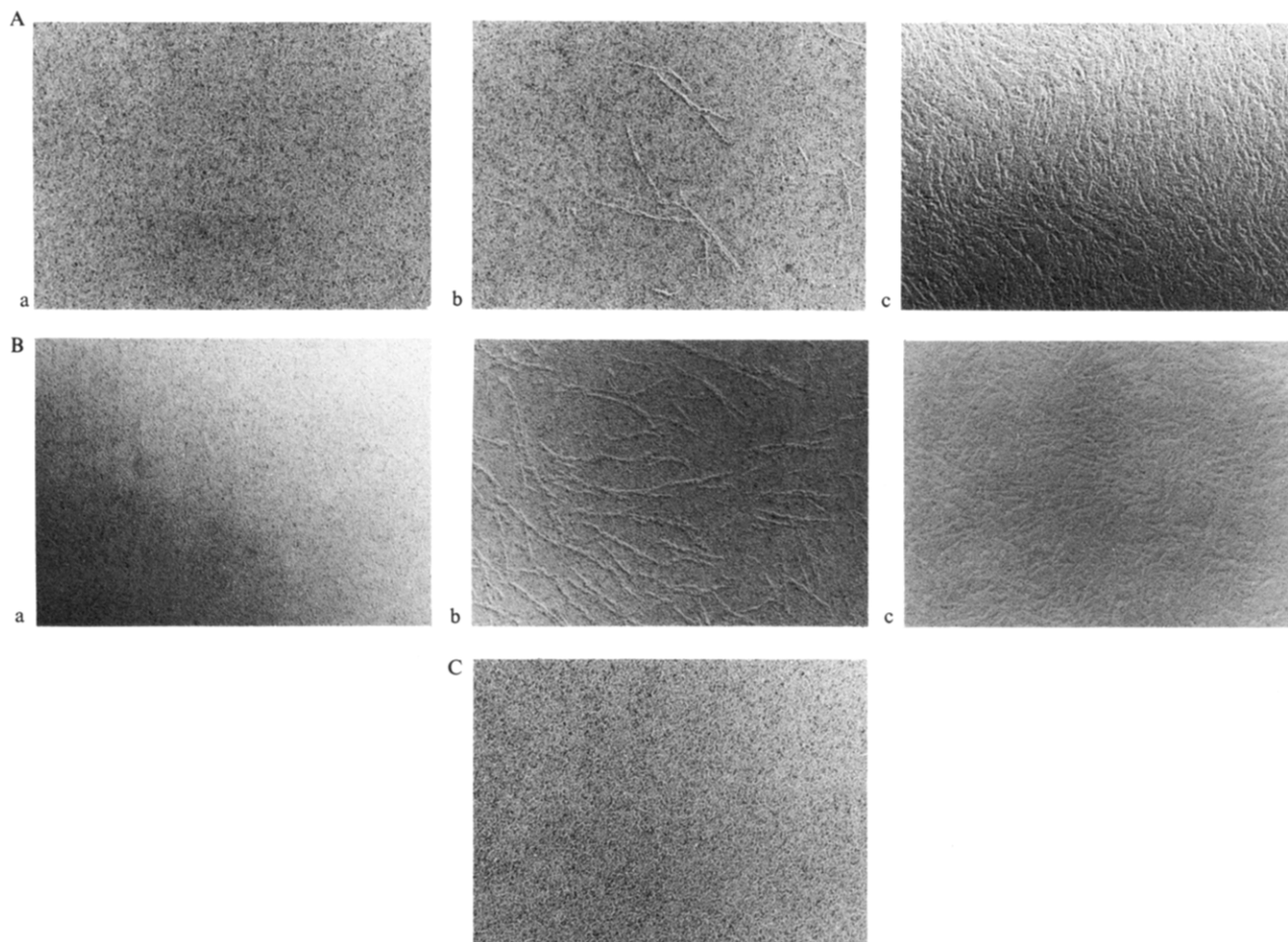


Figure 10. Transmission electron micrographs (magnification 67K) of (A) poly-4-BCMU and (B) poly-3-BCMU taken (a) in the expanded monolayer region, (b) in the transition region, and (c) in the condensed bilayer region (12 dyn/cm). For comparative purposes a blank (C) is included. The width of the rodlike domains in the transition region (80–150 Å) provides a magnification guide.

energy close to 470 nm we could obtain resonant enhancement of the Raman-active vibration of the coil conformation of poly-4-BCMU. In this case the C=C stretching mode occurs at 1532 cm^{-1} . Although this frequency is higher (5 cm^{-1}) than the corresponding one from the bilayer (for the same excitation wavelength), one should recall² the interaction energy between monomolecular layers of the polymer within the region of the plateau. Such interactions may well alter the conformation of an energetically unfavorable coil form to some degree, causing a shift in the frequency of backbone vibrations.

In conclusion, our observations are consistent with a monolayer–bilayer transition of a poly-4-BCMU LB film on a water subphase. Thus they show that the bilayer film of poly-4-BCMU is a mixed structure, consisting of the polymer in both a coil and a rodlike conformation. This conclusion has been further verified in additional studies of poly-4-BCMU LB multilayers. These additional studies involved Raman scattering/surface plasmon wave spectroscopy and have been published elsewhere.¹¹

(e) Transmission Electron Microscopy. Transmission electron microscopy (TEM) of monomolecular films transferred to solid substrates can provide a detailed, well-resolved image of the surface topography of such monolayers.^{12,13} The results of such a study for both poly-4-BCMU and poly-3-BCMU at four surface pressures are shown in the micrographs in Figure 10. For films transferred in the expanded state, a uniform, smooth surface texture is observed. Once into the transition region, how-

ever, distinct rodlike domains are clearly visible for both polymers, those of poly-4-BCMU being less numerous but better resolved than those of poly-3-BCMU. The approximate dimensions of the domains are as follows: length, 800–4000 Å; width, 80–150 Å; height, 10–30 Å. The height was calculated from the domain shadow width and the known Pt shadowing angle.

Just beyond the end of the transition region, into the condensed state, the domains appear much closer together and with increasing surface pressure become increasingly compact so as to give a surface that, while having a rough texture, is also more uniform. Since the appearance of the rodlike domains coincides with the appearance of the red (blue) form in the visible absorption spectra for poly-4-BCMU (poly-3-BCMU), in the transition region and beyond, we interpret the domains to be intramolecular, hydrogen-bonded, red rod (blue rod) conformers and the surrounding film between domains to be amphiphatic yellow coil conformers.

(f) Solid Substrate Effects. The effect of a hydrophobic low-energy, alkylated glass surface in determining the conformation of adjacent poly-4-BCMU and poly-3-BCMU monolayers was investigated by horizontally lifting monomolecular films of these polymers onto such substrates. It was found that this approach, rather than a vertical lift, gave a near ideal deposition ratio with a hydrophobic–hydrophobic contact. The visible absorption spectra of monolayers of both poly-4-BCMU and poly-3-BCMU lifted onto alkylated glass substrates at pressures approximately 1 dyn/cm below π_c are shown in Fig-

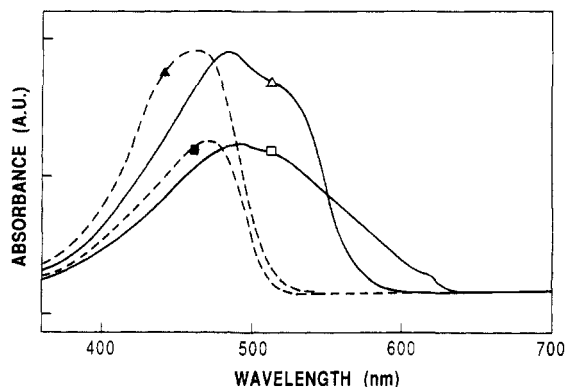


Figure 11. Visible adsorption spectra of monolayers (pretransition region) transferred to hydrophobic, low-energy, alkylated glass surfaces of poly-4-BCMU (Δ) and poly-3-BCMU (\square). The corresponding spectra of these polymers obtained from films transferred to hydrophilic glass supports are shown for comparison: (Δ) poly-4-BCMU and (\bullet) poly-3-BCMU.

ure 11. In the case of poly-4-BCMU the spectrum clearly shows both the red form (525 nm) and a modified yellow form (465 \rightarrow 485 nm), quite different from that in Figure 8 for expanded-state poly-4-BCMU on hydrophilic glass. Poly-3-BCMU shows a similar but different trend toward a more ordered form in which the yellow coil is modified (475 \rightarrow 490 nm) and there are peaks at both 515 and 615 nm. For both polymers the hydrophobic, low-energy substrate clearly has a greater ordering effect upon the conjugated backbone conformation than a hydrophilic, high-energy glass substrate. Interestingly, TEM examination of expanded-state monolayers of poly-4-BCMU and poly-3-BCMU lifted onto hydrophobic substrates showed only a smooth, uniform surface very similar to that obtained by using hydrophilic (mica) substrates. The induced partial coil to rod conversion brought about via hydrophobic substrates apparently is not accompanied by significant displacement of film molecules from their two-dimensional array, such as is the case for a surface pressure induced transition (i.e., compression to less than 100 $\text{\AA}^2/\text{residue}$).

(g) Aqueous Subphase Effects. The repeat units of BCMU polymers include two side groups, each of which has a urethane linkage ($-\text{OC}(\text{O})\text{NH}-$) and an ester group, which together make up the hydrophilic polar group. Polypeptides also consist of repeat units that include urethane linkages, here composing the backbone of the polymer rather than the side groups. Both types of polymers, however, share the fact that hydrogen bonding involving urethane groups plays a key role in determining the conformation of the polymer backbone. It has been shown that both pH changes and the presence of ions such as Ca^{2+} can have a significant effect upon the nature of hydrogen bonding in monolayers of biological systems and in particular monolayers of polypeptides.^{14,15} Therefore the effects of both increased pH (5.6 \rightarrow 12.5) and Ca^{2+} ion content (10^{-3} M CaCl_2) of the water subphase on the π -A isotherms of poly-4-BCMU and poly-3-BCMU were investigated. The results are shown in Figure 12.

The effect of increased pH alone is seen to expand the entire poly-4-BCMU isotherm, while expanding only the condensed state of poly-3-BCMU but with a slight condensing effect on its expanded state. The transition pressure of both polymers was raised by about 1 dyn/cm. Adding CaCl_2 to the strongly basic subphase is seen to dramatically condense both polymers' expanded and condensed states while leaving their transition pressures essen-

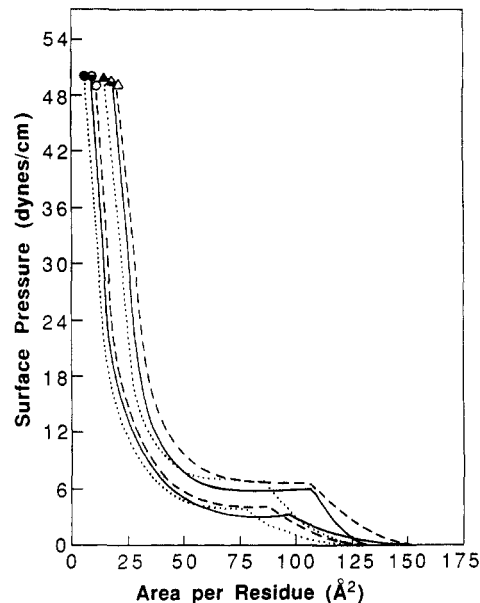


Figure 12. Aqueous subphase effects on the surface pressure/area per residue isotherms of poly-4-BCMU and poly-3-BCMU. The effect of increasing pH (12.5) on poly-4-BCMU (Δ) and poly-3-BCMU (\circ). The effect of increased pH (12.5) and added Ca^{2+} (10^{-3} M CaCl_2) on poly-4-BCMU (\blacktriangle) and poly-3-BCMU (\bullet). The isotherms of both polymers on a neutral aqueous subphase (pH 5.6) are shown for comparison: poly-4-BCMU (Δ) and poly-3-BCMU (\circ).

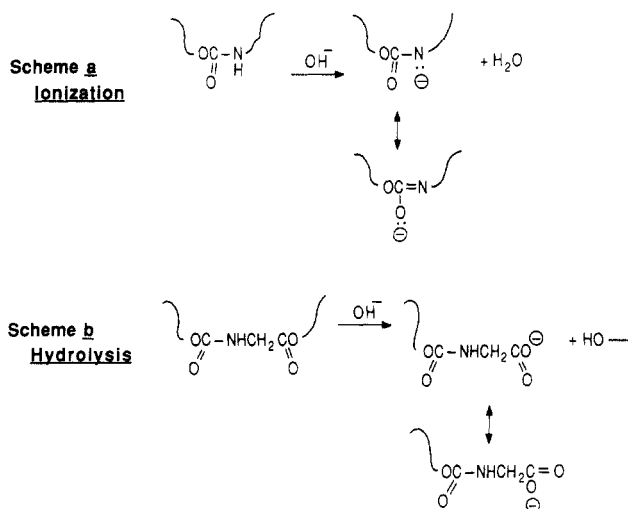


Figure 13. Possible mechanisms to explain the effects of increasing pH and added Ca^{2+} on poly-3-BCMU and poly-4-BCMU. Scheme a, ionization alone; scheme b, hydrolysis alone.

tially unaffected. These results can be rationalized in terms of the polar groups' reactivity toward ionization and hydrolysis in alkaline media, followed by their attraction toward a doubly charged cation such as Ca^{2+} . Figure 13 shows two proposed ionization and hydrolysis products of the BCMU side groups. In scheme a, ionization by abstraction of one proton results in a negatively charged side group having the same chain length as the unionized form. This would therefore result in a mutual repulsion between ionized side groups and could explain the overall expansion effect seen for poly-4-BCMU at pH 12.5. Scheme b, however, involving hydrolysis of the end ester group, would both negatively charge and shorten the length of the side group, which may explain the net condensation of poly-3-BCMU's expanded state. Since the expanded state of poly-3-BCMU is thought to be more convoluted and to penetrate the subphase more than that

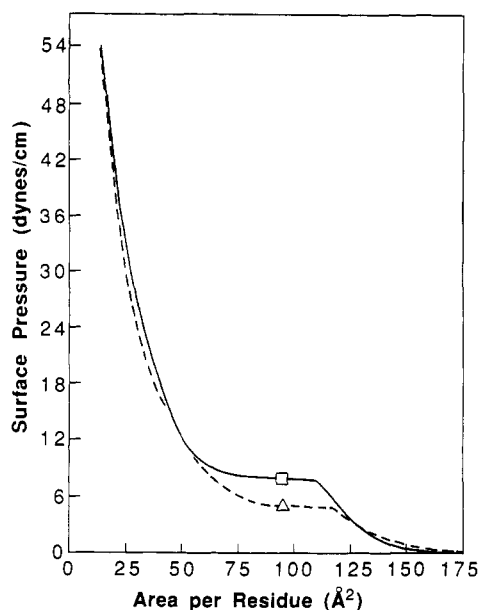


Figure 14. Surface pressure versus area per residue isotherms at 24 °C on 3.0 M NaCl aqueous subphases of poly-3-BCMU (Δ) and poly-4-BCMU (\square).

of poly-4-BCMU,² the greater accessibility of poly-3-BCMU's polar groups to subphase ions could favor hydrolysis (scheme b) in preference or, more likely, in addition to ionization (scheme a). Poly-4-BCMU's more interfacially located polar groups may disfavor hydrolysis over simple proton abstraction, leading to ionization alone or at least a predominance of ionization. The increased transition pressure of both polymers can be seen as being due to an increased polymer-subphase interaction because of the charging of the side groups.

The large condensation of both polymers by the addition of Ca^{2+} is clearly due to the ability of a doubly charged cation to attract two single negative charges, thereby pulling together side groups from either the same or different repeat units along the polymer chain. A comparison of the decreased area per residue of the transition onset of both polymers shows that each polymer exhibits an approximately 20% condensation on a pH 12.5, $\text{Ca}^{2+} = 10^{-3}$ M subphase when compared to a similar film on a substrate of pure water (pH 5.6).

While the effect of the ionic strength (i.e., NaCl) of the subphase can already be seen in the determination of the MW of high and low MW poly-4-BCMU samples, its effect upon the entire isotherm of medium MW poly-4-BCMU and poly-3-BCMU samples is also of interest. The π -A isotherms of poly-4-BCMU and poly-3-BCMU

on a 3.0 M NaCl subphase at 24 °C are shown in Figure 14. While both polymers independently show expansion and increased transition pressures when compared to identical films on pure water,² it can be seen that, on a 3 M salt subphase, both expanded and condensed regions of the π -A isotherms of both polymers are approximately coincident. This gives weight to our prediction that there is greater subphase penetration in the case of poly-3-BCMU than there is for poly-4-BCMU, since exclusion of polymer segments from the salt subphase and their relocation at the air/water interface should then give expanded and condensed regions of the π -A isotherms that are nearly identical for both polymers. That the transition region pressures are different is presumably due to persistent slight differences in behavior of the two polymers and to the high sensitivity of such transitions to minor differences between the polymers. Clearly the subphase composition can have significant effects on the interfacial conformation of poly-3-BCMU and poly-4-BCMU monolayers at the air/water interface.

Acknowledgment. This work was supported by the Air Force Office of Scientific Research, Contract F4962087C0042. We also express our appreciation to Dr. T. M. Szczesny of the SUNY Buffalo Anatomy Department for assistance with the transmission electron microscope studies and to Carol Bonnas for assistance in the typing of this manuscript.

References and Notes

- (1) Biegajski, J. E.; Burzynski, R.; Cadenhead, D. A.; Prasad, P. N. *Macromolecules* **1986**, *19*, 2457.
- (2) Biegajski, J. E.; Cadenhead, D. A.; Prasad, P. N. *Langmuir* **1988**, *4*, 689.
- (3) Chance, R. R.; Patel, G. N.; Witt, J. D. *J. Chem. Phys.* **1979**, *71*, 206.
- (4) Patel, G. N.; Chance, R. R.; Witt, J. D. *J. Chem. Phys.* **1979**, *70*, 4387; *J. Polym. Sci., Polym. Lett. Ed.* **1978**, *16*, 607.
- (5) Patel, G. N.; Walsh, E. K. *J. Polym. Sci., Polym. Lett. Ed.* **1979**, *17*, 203.
- (6) Lim, K. C.; Heeger, A. J. *J. Chem. Phys.* **1985**, *82*, 522.
- (7) Schmidt, M.; Wegner, G. *J. Chem. Phys.* **1986**, *84*, 1057.
- (8) Lim, K. C.; Kapitulnik, A.; Zacker, R.; Heeger, A. J. *J. Chem. Phys.* **1986**, *84*, 1058.
- (9) Cadenhead, D. A. *Ind. Eng. Chem.* **1969**, *81*, 22.
- (10) Motomura, K. *Thermodynamics of Interfacial Monolayers. In Adv. Colloid Interface Sci.* **1980**, *12*, 1.
- (11) Huang, X.; Burzynski, R.; Prasad, P. N. *Langmuir* **1989**, *5*, 325.
- (12) Neuman, R. D.; Fereshtekhou, S.; Ovalle, R. *J. Colloid Interface Sci.* **1984**, *101*, 309.
- (13) Ries, H. E., Jr. *Nature* **1979**, *281*, 287.
- (14) Gabrielli, G.; Ferroni, E.; Huggins, M. L. *Progr. Colloid Polym. Sci.* **1975**, *58*, 201.
- (15) Gabrielli, G.; Baglioni, P.; Fabbrini, A. *Colloids Surf.* **1981**, *38*, 147.